

Field-Effect Josephson Diode via Asymmetric Spin-momentum-locking States

Pei-Hao Fu^{1,2,3,*}, Yong Xu^{1,5}, Shengyuan A. Yang^{2,4}, Ching Hua Lee^{3,†}, Yee Sin Ang^{2,‡} and Jun-Feng Liu^{1§}

¹*School of Physics and Materials Science, Guangzhou University, Guangzhou 510006, China*

²*Science, Mathematics and Technology, Singapore University of Technology and Design, Singapore 487372, Singapore*

³*Department of Physics, National University of Singapore, Singapore 117542*

⁴*Research Laboratory for Quantum Materials, Singapore University of Technology and Design, Singapore 487372, Singapore and*

⁵*Institute of Materials, Ningbo University of Technology, Ningbo 315016, China*

Recent breakthroughs in Josephson diodes dangle the possibility of extending conventional non-reciprocal electronics into the realm of superconductivity. While a strong magnetic field is recognized for enhancing diode efficiency, it concurrently poses a risk of undermining the essential superconductivity required for non-dissipative devices. To circumvent the need for magnetic-based tuning, we propose a field-effect Josephson diode based on the electrostatic gate control of finite momentum Cooper pairs in asymmetric spin-momentum-locking states. We propose two possible implementations of our gate-controlled mechanism: (i) a topological field-effect Josephson diode in time-reversal-broken quantum spin Hall insulators; and (ii) semiconductor-based field-effect Josephson diodes attainable in current experimental setups involving a Zeeman field and spin-orbit coupling. Notably, the diode efficiency is highly enhanced in the topological field-effect Josephson diode because the current carried by the asymmetric helical edge states is topologically protected and can be tuned by local gates. In the proposed Josephson diode, the combination of gates and asymmetric spin-momentum-locking nature is equivalent to that of a magnetic field, thus providing an alternative electrical operation in designing nonreciprocal superconducting devices.

Introduction.- Electronic technologies rely heavily on non-reciprocal charge-transport semiconducting devices such as diodes, alternating-to-direct current converters, and transistors^{1–4}. However, dissipation is inevitable in such devices due to their finite resistance⁵. Superconducting diodes^{6,7} in noncentrosymmetric superconductor^{8–20} and Josephson junctions^{21–39} are promising dissipationless non-reciprocal devices that manifest in direction-selective critical supercurrents, i.e. $I_{c+} \neq I_{c-}$ with $I_{c+/ -}$ is the critical supercurrents in positive/negative direction. When an external applied current lies between I_{c-} and I_{c+} , the transport is dissipationless in one direction due to Cooper-pair formation, while dissipative in the opposite direction [Fig. 1 (a)]. The extent of non-reciprocity is characterized by the diode efficiency,

$$\eta = \frac{I_{c+} - I_{c-}}{I_{c+} + I_{c-}}, \quad (1)$$

and $\text{sign}(\eta)$ defines the diode polarity. Numerous theoretical findings^{41–72} in topological insulators^{49,51,66–69}, semiconductors⁷⁰ and supercurrent interferometers^{61,62}, have suggested superconducting diodes as potential building blocks for high-performance superconducting circuits.

Simultaneously breaking inversion and time-reversal symmetry (TRS) is necessary for superconducting diode effect^{73–75}. The requisite non-reciprocity arises from an additional unidirectional supercurrent carried by finite momentum Cooper pairs resulting from breaking both symmetries^{60,76–78}. To break inversion symmetry, a nuanced device design is essential where the diode efficiency is sensitive to structural parameters²⁰, and challenging to tune once a device is fabricated. Thus, in most ex-

periments, superconducting diode effects are activated and manipulated by external magnetic fields, a typical method for breaking TRS. Unfortunately, superconductivity will ultimately be impaired by sufficiently high magnetic fields, thereby fundamentally limiting their applications⁷⁹. Attention then is drawn to magnetic-field-free superconducting diodes^{19,20,35–40}, where TRS is broken by intrinsic magnetism. However, external magnetic fields are still necessary for diode-on/off and polarity-switching³⁷. As such, an all-electrically-controlled superconducting diode is still under demand, which enhances the flexibility in operating integrated superconducting circuits.

This work proposes a new mechanism for an all-electrically-controlled Josephson diode, wherein supercurrents are carried by asymmetric spin-momentum-locking states (ASMLSs) characterized by electrons with opposite spins counter-propagating with different velocities [Fig. 1]. Specifically, we show that the combination of asymmetry and gate voltage in the superconducting leads plays an equivalent role as a magnetic field to the Cooper pairs. This enables the construction of an all-electrically controllable Josephson diode circumventing magnetic control. Hence, the proposed device can be termed as a *field-effect Josephson diode* (FEJD).

Gate-tunable Cooper-pair momentum.- To illustrate how gate-tunable Cooper-pair momentum arises in ASMLSs and its crucial role in FEJDs, we employ a representative 2-component ASMLS Hamiltonian h_0 , with a Zeeman field m along the spin-polarized axis \hat{z} and electrical potential V :⁸⁰

$$h_0(k_x) = \hbar v_0(\sigma_z + t\sigma_0)k_x + m\sigma_z - V\sigma_0, \quad (2)$$

where v_0 is the Fermi velocity, σ_z and σ_0 are the z -Pauli

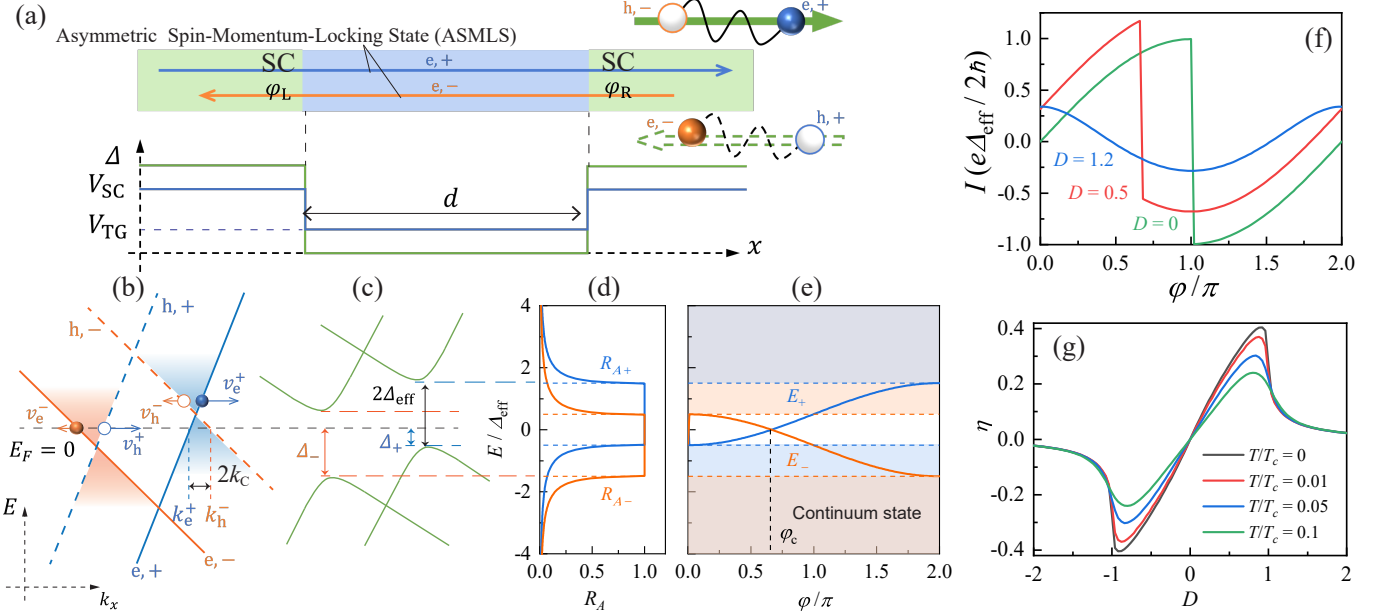


FIG. 1. Mechanism of FEJD mediated by ASMLSSs. (a) FEJD schematics, where the rightward-flowing dissipationless (leftward-flowing dissipative) current, labeled by solid (dashed) green arrow, is carried by Cooper pairs (unpaired carriers) formed by spin-up (spin-down) electrons and spin-down (spin-up) holes represented by blue (orange) solid and hollow circles, respectively. FEJD is controlled by super gates (V_{SC}) and tunneling gate (V_{TG}) applied to superconducting (SC) leads with an order parameter Δ and central normal region with a length d , respectively. (b) and (c): ASMLS dispersion, (b) without and (c) with Δ . In (b), solid (dashed) blue/orange lines represent spin-up/down electrons (holes) dispersion. Velocity of spin-up (spin-down) quasiparticles are $v_{e/h}^{+(-)}$ as denoted by the length of the arrows. FEJD occurs due to the gate-tunable Cooper-pair momentum k_C [Eq. (4)] that causes Doppler energy shift D and spin-dependent SC gaps below $E_F = 0$ as $\Delta_{\pm} = \Delta_{\text{eff}}(1 \mp D)$ in (c). (d-g) are transport characteristics of FEJD with $\hbar v_0 = 1 = \Delta$, $t = 0.1$, and $D = 0.5$. (d) Asymmetric energy-resolved Andreev reflection probabilities, where the unit-probability energy regime corresponds to ABS spectra in (e) with $\varphi_c = 2 \cos^{-1} D$. ABS accompanied by continuum states contribute to supercurrent [Eq. (9)] in (f). The latter solely depends on D resulting in a gate-tunable diode efficiency in (g).

matrix and identity matrix in spin space. To induce asymmetry in the spin-momentum locking, the $tk_x\sigma_0$ term ($0 < t < 1$) tilts the dispersion [Fig. 1(b)], resulting in distinct spin-dependent counter-propagating velocities, i.e. $v_e^\sigma = v_0(\sigma + t)^{80}$ where $\sigma = \pm 1$ denotes the two opposite spins.

Systems described by Eq. (2) are suitable candidates for FEJD. The spin-momentum locking from the $k_x\sigma_z$ term breaks inversion symmetry while the asymmetry induced by tk_x breaks TRS, which is usually achieved through the Zeeman field m^{80} . The simultaneous breaking of both symmetries indicates the possibility of realizing the Josephson diode without a Zeeman field.

To achieve FEJDs, a prerequisite ingredient is gate-tunable Cooper pair momentum. This is modeled through the Bogoliubov-de Gennes (BdG) Hamiltonian^{80,81}

$$H_{\text{BdG}} = \begin{pmatrix} h_0(k_x) & -i\Delta\sigma_y \\ i\Delta\sigma_y & -[h_0(-k_x)]^* \end{pmatrix}, \quad (3)$$

in Nambu space, where Δ is the proximity-induced s -wave superconducting (SC) order parameter. A non-

vanishing Cooper pair momentum^{60,80}

$$k_C = \frac{1}{2}(k_h^{-\sigma} - k_e^\sigma) = \frac{1}{\hbar v_0} \frac{tV + m}{1 - t^2}, \quad (4)$$

results from the net Fermi momentum between holes $k_h^{-\sigma}$ and electrons k_e^σ [Fig. 1(b)] with $k_{e(h)}^\sigma = +(-)(V - \sigma m)/[\hbar v_0(\sigma + t)]$ obtained by the electron and hole block dispersion in Eq. (3)⁸⁰.

The Cooper-pair momentum shifts the SC-gap center from $E = E_F = 0$ to a finite energy, known as the Doppler energy shift⁶⁰,

$$D = (1 - t^2) \frac{\hbar v_0 k_C}{\Delta_{\text{eff}}} = \frac{tV + m}{\Delta_{\text{eff}}}, \quad (5)$$

in the unit of effective SC gap $\Delta_{\text{eff}} = \sqrt{1 - t^2}\Delta^{80}$. As a result, the energy of right-propagating (left-propagating) spin-up (spin-down) states increases (decreases), manifesting as spin-dependent SC gaps $\Delta_\sigma = \Delta_{\text{eff}}(1 - \sigma D)$ below $E_F = 0$ [Fig. 1(c)]⁸⁰.

From Eq. (4) and (5), the joint effect of the asymmetry and gate voltage, tV , is seen to play the same role as the Zeeman field m , leading to gate-tunable Cooper-pair momentum k_C .

Field-effect Josephson diode (FEJD).- Having explained how gate-tunable Cooper-pair momentum k_C can be achieved, we next describe how they give rise to FEJDs with gate-controlled diode efficiency η . Our prototypical FEJD setup, based on Eq. (3), is schematically illustrated in Fig. 1(a) with super gates (V_{SC}) applied to the left ($x < 0$) and right ($x > d$) SC leads and a tunneling gate (V_{TG}) applied to the middle non-SC region of length d ³⁹. The SC gap and electrical potential profiles are $\Delta(x) = \Delta [e^{i\varphi_L} \Theta(-x) + e^{i\varphi_R} \Theta(x-d)]$ and $V(x) = V_{SC} \Theta(x^2 - xd) + V_{TG} \Theta(xd - x^2)$ with macroscopic SC phases $\varphi_{L/R}$ in the left/right SC leads.

Here the supercurrent is carried by ASMLSSs [Fig. 1(a)]. Because of spin-momentum locking, the spin-up (spin-down) electrons are right-propagating (left-propagating), and undergo spin-flip Andreev reflections at the interfaces with the SC regions. Considering the scattering matrix at these interfaces⁸⁰, the asymmetric BdG dispersion [Fig. 1(c)] in the SC regions results in asymmetric Andreev reflection probabilities $R_{A,\pm}(E) \neq R_{A,\pm}(-E)$ for a quasiparticle of energy E , as shown in Fig. 1(d), where

$$R_{A,\pm}(E) = |e^{-i\theta_\pm}|^2, \quad (6)$$

$$\theta_\pm = \begin{cases} \cos^{-1}\left(\frac{E}{\Delta_{\text{eff}}} \mp D\right) & , \left|\frac{E}{\Delta_{\text{eff}}} \mp D\right| < 1 \\ -i \cosh^{-1}\left(\frac{E}{\Delta_{\text{eff}}} \mp D\right) & , \left|\frac{E}{\Delta_{\text{eff}}} \mp D\right| > 1 \end{cases}. \quad (7)$$

In the $\left|\frac{E}{\Delta_{\text{eff}}} \mp D\right| < 1$ case, $R_{A,\pm} = 1$ identically. This asymmetry crucially arises from the nonzero Doppler energy shift D and gives rise to spin-dependent Andreev bound states (ABSs) spectra, which, in the short junction limit of $d \ll \hbar v_0 / \Delta$,⁸⁰ is

$$E_\pm(\varphi) / \Delta_{\text{eff}} = \pm D \mp \text{sgn}[\sin(\varphi/2)] \cos(\varphi/2), \quad (8)$$

as plotted in Fig. 1(e), where $\varphi = \varphi_R - \varphi_L$ is the phase difference between two SC leads. Importantly, gapless ABSs occurs when $\varphi = \varphi_c = 2 \cos^{-1} D$.

Through the scattering matrix formalism^{80,82,83}, we obtain the zero-temperature supercurrent,

$$I(\varphi) = \begin{cases} I_{\text{ABS}}(\varphi) + I_{\text{cont}} & , |D| < 1 \\ (e\Delta_{\text{eff}}/2\hbar) \text{sign}(D) \Gamma(\varphi) & , |D| \geq 1 \end{cases}, \quad (9)$$

where $I_{\text{ABS}}(\varphi) = (e\Delta_{\text{eff}}/2\hbar) \text{sgn}\{\cos(\varphi/2) - D \text{sgn}[\sin(\varphi/2)]\} \sin(\varphi/2)$ and $I_{\text{cont}} = (e\Delta_{\text{eff}}/2\hbar) 2D/\pi$ arising from the ABSs and continuum states, respectively. Particularly, when $m = 0$, $I_{\text{cont}} = etV_{SC}/(\pi\hbar)$ is solely gate-induced. For $|D| \geq 1$, both contributions become inseparable since φ_c disappears, and the continuous expression is $\Gamma(\varphi) = (2/\pi) \left\{ |D| - \sqrt{D^2 - 1} - \sin(\varphi/2) \tan^{-1} \left[\frac{\sin(\varphi/2)}{\sqrt{D^2 - 1}} \right] \right\}$.

As evident in Fig. 1(f), $I(\varphi)$ exhibits a sharp discontinuity at $\varphi = \varphi_c$ for $D < 1$. This has significant implications for the dissimilarity of the direction-selective

critical Josephson currents, which are defined as the extrema $I(\varphi)$ i.e. $I_{c+} = \max_\varphi I(\varphi)$ and $I_{c-} = |\min_\varphi I(\varphi)|$. In particular, for $0 < D < 1$, the current reverses at $\varphi = \varphi_c$ and $I_{c+} = I(\varphi_c)$, $I_{c-} = -I(\pi)$. Intuitively, we expect the ABSs contributions to $I_{c\pm}$ by the right-moving spin-up electrons and the left-moving counterpart to be different because of the different gaps experienced, i.e. $I_{\text{ABS}}(\varphi_c) \propto \Delta_+ < |I_{\text{ABS}}(\pi)| \propto \Delta_-$. Indeed, in the $D \ll 1$ limit, the I_{cont} contribution is seen to enhance (suppress) the right-moving (left-moving) current, leading to $I_{c\pm} = e\Delta_{\text{eff}}/(2\hbar)(1 \pm 2D/\pi)$.

All in all, by substituting $I_{c\pm}$ into Eq. (1), we obtain the diode efficiency

$$\eta = \frac{D}{|D|} \times \begin{cases} \frac{4|D|/\pi + \sqrt{1-D^2-1}}{\sqrt{1-D^2+1}} & , |D| < 1 \\ \frac{2(|D|-\sqrt{D^2-1})-\cot^{-1}\sqrt{D^2-1}}{\cot^{-1}\sqrt{D^2-1}} & , |D| > 1 \end{cases} \quad (10)$$

which solely depends on D as shown in Fig. 1(g), alongside results at nonzero temperatures T . Notably, for $T = 0$, the diode efficiency reaches a theoretical maximum of $|\eta| \sim 40.5\%$ at $|D| = 4\pi/(4 + \pi^2) \approx 0.906$, which is comparable to the value obtained by applying a magnetic field^{60,67}. However, it gradually vanishes as $|D|$ gets larger, since in the $|D| \gg 1$ limit, the extrema of the current $\lim_{|D| \gg 1} I(\varphi) = e\Delta_{\text{eff}}/(hD) \cos \varphi$ becomes symmetric, as shown in Fig. 1(f).

The exclusive functional dependence of the diode efficiency η on the Doppler energy shift $D = (tV_{SC} + m)/\Delta_{\text{eff}}$ [Eq. (5)] implies that the gate control voltage V_{SC} plays, in the presence of asymmetry t , an indistinguishable role from that of the Zeeman field m ⁶⁰. Hence, the diode efficiency can be completely gate-controlled; for instance, in the $m = 0$ and $D \ll 1$ limit, $\eta \propto D \propto tV_{SC}$ ⁸⁰.

Topological FEJDs.- A potential platform for a FEJD is a TRS-broken quantum spin Hall insulator (QSHI)^{84–86} with well-defined spin-Chern number^{87–89}, which possesses anisotropic topologically protected helical edge states as the ASMLSSs carrying the supercurrent^{90–96}.

A general ansatz Hamiltonian for TRS-broken QSHI is^{84–86,97}, $H_{\text{QSHI}}(\mathbf{k}) = (M_\gamma - B_\gamma |\mathbf{k}|^2) \sigma_0 \tau_z + M_\alpha \sigma_z \tau_0 + M_\beta \sigma_z \tau_z + \hbar v_0 (\boldsymbol{\sigma} \cdot \mathbf{k}) \tau_x + \hbar v_0 (\boldsymbol{\sigma} \times \mathbf{k})_z \tau_y$ with $\boldsymbol{\tau}$ (τ_0) the Pauli (identity) matrices in sublattice space and $\mathbf{k} = (k_x, k_y)$. With $M_\alpha = 0.1M_\gamma = 0.2B_\gamma = 0.2$ and $M_\beta = 0$, anisotropic helical edge states exist⁸⁴. Our numerical results⁸⁰ show that the FEJD remain gate-controlled as long as the anisotropic helical edge states remain, even with an effective Zeeman field ($M_\beta \neq 0$)⁹⁸, modifies the bulk band gap⁹⁵ and hybridized the edge states invariably induces by TRS-breaking perturbation.

The top (t) and bottom (b) edges of a QSHI each constitute an individual FEJD, with gates $V_{SC}^{s=t/b}$ and Zeeman fields $m^s = \pm m$ ⁸⁴. It is straightforward to apply Eqs. (9–10) to calculate each edge current $I^s(\varphi)$ and the diode efficiency η ⁸⁰.

The advantage of this topological implementation is to enhance η through interference⁶¹ between two topological

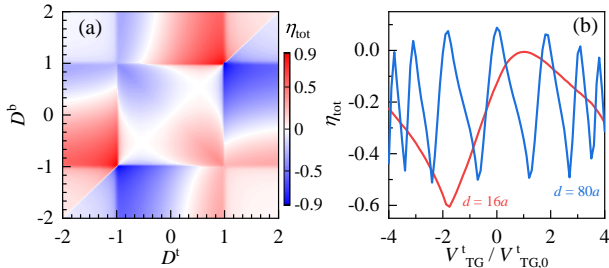


FIG. 2. Diode efficiency of a topological FEJD through two-edge interference in a TRS-broken QSHI. (a) The interfering diode efficiency maximized to $|0.9|$ when $|D^t/b| \gtrsim 1$ and $|D^b| \lesssim 1$. Other parameters are the same as those in Fig. 1. (b) The V_{TG}^t -controlled oscillating diode efficiency originates from the phase difference between two currents. $a = 1$ is the lattice constant and $V_{\text{TG}}^b = 0$.

edge currents. The combined efficiency⁸⁰

$$\eta^{\text{tot}} = \begin{cases} \frac{\sqrt{1-(D^t)^2}-\sqrt{1-(D^b)^2}+\frac{2}{\pi}(D^t-D^b)}{\sqrt{1-(D^t)^2}+\sqrt{1-(D^b)^2}}, & 0 \leq D^t \leq 1 \\ \frac{Z_-+2(D^t-D^b)-\sqrt{(D^t)^2-1}}{Z_+}, & D^t > 1 \end{cases}, \quad (11)$$

with $0 \leq D^b < 1$ and $Z_{\pm} = \frac{\pi}{2} - \cot^{-1}(\sqrt{(D^t)^2 - 1}) \pm \sqrt{1 - (D^b)^2}[\frac{\pi}{2} + \tan^{-1}(\sqrt{\frac{1-(D^b)^2}{(D^t)^2-1}})]$ shows that when $|D^t| \gtrsim 1$ and $|D^b| \lesssim 1$, the diode efficiency is enhanced up to 90%, much higher than the one in individual edge [Fig. 2(a)]. Notably, this enhancement is unattainable through a magnetic field^{90–92}, which cancels⁹² continuum-state currents with $D^t = D^b$, thereby leading to a vanishing diode effect.

The interference between two ASMLS currents also leads to a V_{TG} -tunable η . In a finite-length junction, $d > \hbar v_0 \Delta$, a phase difference between two interfering ASMLS is accumulated⁸⁴, which gives rise to $I^{\text{tot}} = \sum_s I^s(\varphi + \varphi_{\text{TG}}^s)$ with $\varphi_{\text{TG}}^s = 2tV_{\text{TG}}^s d [\hbar v_F (1-t^2)]^{-1}$ and $\varphi_{\text{TG}}^s(V_{\text{TG},0}) = 2\pi$. The η oscillates strongly with V_{TG} [Fig. 2(b)], as numerically computed with the lattice Green's function technique^{80,99,100} with $\Delta(T) = \Delta(0) \tanh(1.74\sqrt{T_c/T - 1})$, $\Delta(0) = 0.01M_\gamma$, and $T/T_c = 0.01$.

FEJD in semiconductor.– The mechanism of realizing a FEJD using ASMLSs is also attainable in semiconductors, which provides an alternative theoretical explanation on a recent experiment³⁹.

The ASMLSs occur in semiconductors due to the interplay between the Zeeman field and the spin-orbit interaction (SOI). The general Hamiltonian is^{101,102} $H_{2D}(\mathbf{k}) = t_0 a^2 |\mathbf{k}|^2 - V + \alpha_R a (\boldsymbol{\sigma} \times \mathbf{k})_z + \mathbf{m} \cdot \boldsymbol{\sigma}$ where α_R describes the Rashba SOI and $\mathbf{m} = m_0(\cos \varphi_m, \sin \varphi_m, 0)$ is the in-plane Zeeman field. When $\varphi_m \neq n\pi$ ($n \in \mathbb{Z}$), dispersion of $H_{2D}(\mathbf{k})$ is shifted in k_x direction. Two pairs of ASMLSs occur near E_F [Fig. 3(a) and (b)]⁸⁰, resembling two edges in TRS-broken QSHIs. Thus, a gate-tunable Cooper-pair momentum is expected in a semiconductor

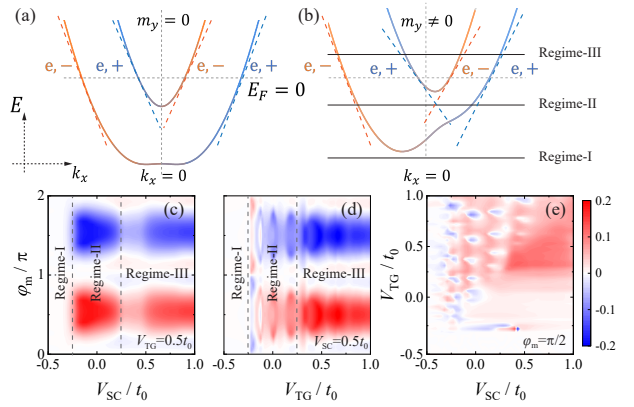


FIG. 3. Mechanism and gate-tunable operation of semiconductor-based FEJD. (a) and (b) show dispersions ($k_y = 0$) of 2D semiconductors with SOI $\alpha_0 = t_0$ ($t_0 = 1$) and Zeeman field $\mathbf{m} = m_0(\cos \varphi_m, \sin \varphi_m, 0)$ with $m_0 = 0.1t_0$. ASMLSs occur around $E_F = 0$ (the dashed grey horizontal lines) when $m_y = m_0 \sin \varphi_m \neq 0$. The diode efficiency in (c-e) is attributed to the ASMLSs in three transport regimes experienced by the systems when sweeping the gates. The parameters are $\Delta(0) = 0.05t_0$, $T/T_c = 0.1$, and $d = 20a$.

based FEJD.

Diode efficiencies of FEJD in the x -direction exhibit three operating regimes depending on the gate-controlled Fermi level⁸⁰ [Fig. 3(c-e)]. In Regimes I/II/III, none/one/two ballistic superconducting channels across the Fermi level [Fig. 3(b)]. η is absent in Regime I and oscillates with V_{TG} in Regime II due to the Fabry-Pérot interference between one ballistic and one tunneling channel [Fig. 3(d)]⁸⁰ resembling the topological implementation in Fig. 2(b).

Although the mechanism of FEJD is shared with the topological FEJD due to the ASMLSs, the gate-operating performance exhibited in Fig. 3(c-e) is not as good as the topological implementation, because of the inevitable back-scattering between $|e, \pm\rangle$ and $|e, \mp\rangle$ due to the parallel spin-orientation component, which is forbidden in QSHI where spin orientation is tightly locked to the momentum.

The formation of ASMLSs also accounts for the dependence of the diode efficiency on the direction of the in-plane Zeeman field. The diode efficiency vanishes when $\varphi_m = n\pi$, because of the symmetric dispersion [Fig. 3(a)]. But when the in-plane Zeeman field is parallel to $k_x \sigma_y$, diode efficiency is maximized since the Cooper-pair momentum is pronounced due to the maximum shift of the dispersion. Although our results are qualitatively consistent with the experiment observations³⁹, there are some deviations in the $\eta - \varphi_m$ relation which only indicates the direction of the pure SOI field and is not a simple sinusoidal function³⁹, but contains higher-harmonic terms⁸⁰.

Discussions and conclusions.– In summary, a mechanism for realizing FEJDs via ASMLSs is proposed. The synergistic effect of ASMLSs and an electric gate

is equivalent to the Zeeman effect, providing access to gate-tunable Cooper-pair momentum and Josephson diode. TRS-broken QSHIs are ideal platforms for topological FEJD. Candidate materials include magnetic-doped QSHIs^{105,106}, MnBi₂Te₄^{107,108}, and WTe₂^{109,110} with typical superconducting proximate gaps in the order from 0.1 meV^{21,78,107,108} to 1 meV^{109,110}. To achieve the optimized diode efficiency with $D \approx 0.91$, electrical potential around 10 meV^{111,112} is required for $t = 0.1$. Corresponding critical currents (~ 10 nA) are experimentally detectable^{27,28}. The semiconductor-based Josephson diode is recently achieved in InSb nanowires³⁹ and expected in InAs^{27–29}. Notably, with ferromagnetic systems³⁷, FEJDs are attainable based on the current technique of magnetic-field-free Josephson diodes.

ACKNOWLEDGMENTS

P.-H. F. thanks Weiping Xu, Shi-Han Zheng, Shuai Li, Jiayu Li, and Jin-Xin Hu for inspiring discussions. P.-H.

F. & Y. S. A. are supported by the Singapore Ministry of Education (MOE) Academic Research Fund (AcRF) Tier 2 Grant (MOE-T2EP50221-0019). C.H.L. is supported by Singapore's NRF Quantum engineering grant NRF2021-QEP2-02-P09 and Singapore's MOE Tier-II grant Proposal ID: T2EP50222-0008. J.-F. L. is supported by the National Natural Science Foundation of China (Grants No. 12174077), the Bureau of Education of Guangzhou Municipality (Grant No. 202255464), and the Natural Science Foundation of Guangdong Province (Grant No. 2021A1515012363).

* peihao_fu@sutd.edu.sg

† phylch@nus.edu.sg

‡ yeesin_ang@sutd.edu.sg

§ phjfliu@gzhu.edu.cn

¹ M. Fruchart, R. Hanai, P. B. Littlewood, and V. Vitelli, Non-Reciprocal Phase Transitions, *Nature* **592**, 363 (2021).

² H. Zhang, T. Chen, L. Li, C. H. Lee, and X. Zhang, Electrical Circuit Realization of Topological Switching for the Non-Hermitian Skin Effect, *Phys. Rev. B* **107**, 085426 (2023).

³ X. Zhao, Y. Xing, J. Cao, S. Liu, W.-X. Cui, and H.-F. Wang, Engineering Quantum Diode in One-Dimensional Time-Varying Superconducting Circuits, *Npj Quantum Inf.* **9**, 59 (2023).

⁴ A. Stegmaier et al., Realizing Efficient Topological Temporal Pumping in Electrical Circuits, arXiv: 2306.15434 (2023).

⁵ S. M. Sze, & M.-K. Lee, *Semiconductor Devices: Physics and Technology* 3rd edn (Wiley, 2012).

⁶ M. Nadeem, M. S. Fuhrer, and X. Wang, The Superconducting Diode Effect, *Nat. Rev. Phys.* **5**, 558 (2023).

⁷ R. Wakatsuki, Y. Saito, S. Hoshino, Y. M. Itahashi, T. Ideue, M. Ezawa, Y. Iwasa, and N. Nagaosa, Nonreciprocal Charge Transport in Noncentrosymmetric Superconductors, *Sci. Adv.* **3**, e1602390 (2017).

⁸ E. Zhang, X. Xu, Y.-C. Zou, L. Ai, X. Dong, C. Huang, P. Leng, S. Liu, Y. Zhang, Z. Jia, X. Peng, M. Zhao, Y. Yang, Z. Li, H. Guo, S. J. Haigh, N. Nagaosa, J. Shen, and F. Xiu, Nonreciprocal Superconducting NbSe₂ Antenna, *Nat. Commun.* **11**, 5634 (2020).

⁹ F. Ando, Y. Miyasaka, T. Li, J. Ishizuka, T. Arakawa, Y. Shiota, T. Moriyama, Y. Yanase, and T. Ono, Observation of Superconducting Diode Effect, *Nature* **584**, 373 (2020).

¹⁰ T. Schumann, L. Galletti, H. Jeong, K. Ahadi, W. M.

Strickland, S. Salmani-Rezaie, and S. Stemmer, Possible Signatures of Mixed-Parity Superconductivity in Doped Polar SrTiO₃ Films, *Phys. Rev. B* **101**, 100503(R) (2020).

¹¹ L. Bauriedl, C. Bäuml, L. Fuchs, C. Baumgartner, N. Paulik, J. M. Bauer, K.-Q. Lin, J. M. Lupton, T. Taniguchi, K. Watanabe, C. Strunk, and N. Paradiso, Supercurrent Diode Effect and Magnetochiral Anisotropy in Few-Layer NbSe₂, *Nat. Commun.* **13**, 4266 (2022).

¹² Y. M. Itahashi, T. Ideue, Y. Saito, S. Shimizu, T. Ouchi, T. Nojima, and Y. Iwasa, Nonreciprocal Transport in Gate-Induced Polar Superconductor SrTiO₃, *Sci. Adv.* **6**, eaay9120 (2020).

¹³ J. Yun, S. Son, J. Shin, G. Park, K. Zhang, Y. J. Shin, J.-G. Park, and D. Kim, Magnetic Proximity-Induced Superconducting Diode Effect and Infinite Magnetoresistance in a van Der Waals Heterostructure, *Phys. Rev. Res.* **5**, L022064 (2023).

¹⁴ Y.-Y. Lyu, J. Jiang, Y.-L. Wang, Z.-L. Xiao, S. Dong, Q.-H. Chen, M. V. Milošević, H. Wang, R. Divan, J. E. Pearson, P. Wu, F. M. Peeters, and W.-K. Kwok, Superconducting Diode Effect via Conformal-Mapped Nanoholes, *Nat. Commun.* **12**, 2703 (2021).

¹⁵ K. Yasuda, H. Yasuda, T. Liang, R. Yoshimi, A. Tsukazaki, K. S. Takahashi, N. Nagaosa, M. Kawasaki, and Y. Tokura, Nonreciprocal Charge Transport at Topological Insulator/Superconductor Interface, *Nat. Commun.* **10**, 2734 (2019).

¹⁶ Y. Wu, Q. Wang, X. Zhou, J. Wang, P. Dong, J. He, Y. Ding, B. Teng, Y. Zhang, Y. Li, C. Zhao, H. Zhang, J. Liu, Y. Qi, K. Watanabe, T. Taniguchi, and J. Li, Nonreciprocal Charge Transport in Topological Kagome Superconductor CsV₃Sb₅, arXiv: 2210.10437 (2022).

¹⁷ M. Masuko, M. Kawamura, R. Yoshimi, M. Hirayama, Y. Ikeda, R. Watanabe, J. J. He, D. Maryenko, A. Tsukazaki, K. S. Takahashi, M. Kawasaki, N. Nagaosa, and Y. Tokura, Nonreciprocal Charge Transport in Topological

- Superconductor Candidate Bi₂Te₃/PdTe₂ Heterostructure, *Npj Quantum Mater.* **7**, 104 (2022).
- ¹⁸ Y. Hou, F. Nichele, H. Chi, A. Lodesani, Y. Wu, M. F. Ritter, D. Z. Haxell, M. Davydova, S. Ilić, O. Glezakou-Elbert, A. Varambally, F. S. Bergeret, A. Kamra, L. Fu, P. A. Lee, and J. S. Moodera, Ubiquitous Superconducting Diode Effect in Superconductor Thin Films, *Phys. Rev. Lett.* **131**, 027001 (2023).
- ¹⁹ J.-X. Lin, P. Siriviboon, H. D. Scammell, S. Liu, D. Rhodes, K. Watanabe, T. Taniguchi, J. Hone, M. S. Scheurer, and J. I. A. Li, Zero-Field Superconducting Diode Effect in Small-Twist-Angle Trilayer Graphene, *Nat. Phys.* **18**, 1221 (2022).
- ²⁰ H. Narita, J. Ishizuka, R. Kawarasaki, D. Kan, Y. Shioota, T. Moriyama, Y. Shimakawa, A. V. Ognev, A. S. Samardak, Y. Yanase, and T. Ono, Field-Free Superconducting Diode Effect in Noncentrosymmetric Superconductor/Ferromagnet Multilayers, *Nat. Nanotechnol.* **17**, 823 (2022).
- ²¹ E. Bocquillon, R. S. Deacon, J. Wiedenmann, P. Leubner, T. M. Klapwijk, C. Brüne, K. Ishibashi, H. Buhmann, and L. W. Molenkamp, Gapless Andreev Bound States in the Quantum Spin Hall Insulator HgTe, *Nat. Nanotechnol.* **12**, 137 (2017).
- ²² J. Diez-Merida, A. Diez-Carlon, S. Y. Yang, Y.-M. Xie, X.-J. Gao, K. Watanabe, T. Taniguchi, X. Lu, K. T. Law, and D. K. Efetov, Magnetic Josephson Junctions and Superconducting Diodes in Magic Angle Twisted Bilayer Graphene, arXiv: 2110.01067 (2021).
- ²³ E. Portolés, S. Iwakiri, G. Zheng, P. Rickhaus, T. Taniguchi, K. Watanabe, T. Ihn, K. Ensslin, and F. K. de Vries, A Tunable Monolithic SQUID in Twisted Bilayer Graphene, *Nat. Nanotechnol.* **17**, 1159 (2022).
- ²⁴ B. Pal, A. Chakraborty, P. K. Sivakumar, M. Davydova, A. K. Gopi, A. K. Pandeya, J. A. Krieger, Y. Zhang, M. Date, S. Ju, N. Yuan, N. B. M. Schröter, L. Fu, and S. S. P. Parkin, Josephson Diode Effect from Cooper Pair Momentum in a Topological Semimetal, *Nat. Phys.* **18**, 1228 (2022).
- ²⁵ B. Turini, S. Salimian, M. Carrega, A. Iorio, E. Strambini, F. Giazotto, V. Zannier, L. Sorba, and S. Heun, Josephson Diode Effect in High Mobility InSb Nanoflags, *Nano Lett.* **22**, 8502 (2022).
- ²⁶ M. Gupta, G. V. Graziano, M. Pendharkar, J. T. Dong, C. P. Dempsey, C. Palmström, and V. S. Pribiag, Gate-Tunable Superconducting Diode Effect in a Three-Terminal Josephson Device, *Nat. Commun.* **14**, 3078 (2023).
- ²⁷ C. Baumgartner, L. Fuchs, A. Costa, S. Reinhardt, S. Gronin, G. C. Gardner, T. Lindemann, M. J. Manfra, P. E. Faria Junior, D. Kochan, J. Fabian, N. Paradiso, and C. Strunk, Supercurrent Rectification and Magnetochiral Effects in Symmetric Josephson Junctions, *Nat. Nanotechnol.* **17**, 39 (2022).
- ²⁸ C. Baumgartner, L. Fuchs, A. Costa, J. Picó-Cortés, S. Reinhardt, S. Gronin, G. C. Gardner, T. Lindemann, M. J. Manfra, P. E. Faria Junior, D. Kochan, J. Fabian, N. Paradiso, and C. Strunk, Effect of Rashba and Dresselhaus Spin-Orbit Coupling on Supercurrent Rectification and Magnetochiral Anisotropy of Ballistic Josephson Junctions, *J. Phys. Condens. Matter* **34**, 154005 (2022).
- ²⁹ A. Costa, C. Baumgartner, S. Reinhardt, J. Berger, S. Gronin, G. C. Gardner, T. Lindemann, M. J. Manfra, D. Kochan, J. Fabian, N. Paradiso, and C. Strunk, Sign Reversal of the Josephson Inductance Magnetochiral Anisotropy and 0- π -like Transitions in Supercurrent Diodes *Nat. Nanotechnol.* **18**, 1266 (2023).
- ³⁰ M. S. Anwar, T. Nakamura, R. Ishiguro, S. Arif, J. W. A. Robinson, S. Yonezawa, M. Sigrist, and Y. Maeno, Spontaneous Superconducting Diode Effect in Non-Magnetic Nb/Ru/Sr₂RuO₄ Topological Junctions, *Commun. Phys.* **6**, 290 (2023).
- ³¹ S. Ghosh, V. Patil, A. Basu, Kuldeep, D. A. Jangade, R. Kulkarni, A. Thamizhavel, and M. M. Deshmukh, High-Temperature Superconducting Diode, arXiv: 2210.11256 (2022).
- ³² J. Chiles, E. G. Arnault, C.-C. Chen, T. F. Q. Larson, L. Zhao, K. Watanabe, T. Taniguchi, F. Amet, and G. Finkelstein, Nonreciprocal Supercurrents in a Field-Free Graphene Josephson Triode, *Nano Lett.* **23**, 5257 (2023).
- ³³ M. Trahms, L. Melischek, J. F. Steiner, B. Mahendru, I. Tamir, N. Bogdanoff, O. Peters, G. Reeht, C. B. Winkelmann, F. von Oppen, and K. J. Franke, Diode Effect in Josephson Junctions with a Single Magnetic Atom, *Nature* **615**, 628 (2023).
- ³⁴ X. Song, S. Suresh-Babu, Y. Bai, D. Golubev, I. Burkova, A. Romanov, E. Ilin, J. N. Eckstein, and A. Bezryadin, Interference, Diffraction, and Diode Effects in Superconducting Array Based on Bismuth Antimony Telluride Topological Insulator, *Commun. Phys.* **6**, 177 (2023).
- ³⁵ T. Golod and V. M. Krasnov, Demonstration of a Superconducting Diode-with-Memory, Operational at Zero Magnetic Field with Switchable Nonreciprocity, *Nat. Commun.* **13**, 3658 (2022).
- ³⁶ F. Zhang, M. T. Ahari, A. S. Rashid, G. J. de Coster, T. Taniguchi, K. Watanabe, M. J. Gilbert, N. Samarth, and M. Kayyalha, Reconfigurable Magnetic-Field-Free Superconducting Diode Effect in Multi-Terminal Josephson Junctions, arXiv: 2301.05081 (2023).
- ³⁷ K.-R. Jeon, J.-K. Kim, J. Yoon, J.-C. Jeon, H. Han, A. Cottet, T. Kontos, and S. S. P. Parkin, Zero-Field Polarity-Reversible Josephson Supercurrent Diodes Enabled by a Proximity-Magnetized Pt Barrier, *Nat. Mater.* **21**, 1008 (2022).
- ³⁸ H. Wu, Y. Wang, Y. Xu, P. K. Sivakumar, C. Pasco, U. Filippozzi, S. S. P. Parkin, Y.-J. Zeng, T. McQueen, and M. N. Ali, The Field-Free Josephson Diode in a van Der Waals Heterostructure, *Nature* **604**, 653 (2022).
- ³⁹ G. P. Mazur, N. van Loo, D. van Driel, J.-Y. Wang, G. Badawy, S. Gazibegovic, E. P. A. M. Bakkers, and L. P. Kouwenhoven, The Gate-Tunable Josephson Diode, arXiv: 2211.14283 (2022).
- ⁴⁰ J. Jiang, M. V. Milošević, Y.-L. Wang, Z.-L. Xiao, F. M. Peeters, and Q.-H. Chen, Field-Free Superconducting Diode in a Magnetically Nanostructured Superconductor, *Phys. Rev. Appl.* **18**, 034064 (2022).
- ⁴¹ S. Hoshino, R. Wakatsuki, K. Hamamoto, and N. Nagaosa, Nonreciprocal Charge Transport in Two-Dimensional Noncentrosymmetric Superconductors, *Phys. Rev. B* **98**, 054510 (2018).
- ⁴² R. Wakatsuki and N. Nagaosa, Nonreciprocal Current in Noncentrosymmetric Rashba Superconductors, *Phys. Rev. Lett.* **121**, 026601 (2018).
- ⁴³ B. Zhai, B. Li, Y. Wen, F. Wu, and J. He, Prediction of Ferroelectric Superconductors with Reversible Superconducting Diode Effect, *Phys. Rev. B* **106**, L140505 (2022).
- ⁴⁴ J. J. He, Y. Tanaka, and N. Nagaosa, A Phenomenological Theory of Superconductor Diodes, *New J. Phys.* **24**,

- 053014 (2022).
- ⁴⁵ H. D. Scammell, J. I. A. Li, and M. S. Scheurer, Theory of Zero-Field Superconducting Diode Effect in Twisted Trilayer Graphene, *2D Mater.* **9**, 025027 (2022).
- ⁴⁶ S. Ilić and F. S. Bergeret, Theory of the Supercurrent Diode Effect in Rashba Superconductors with Arbitrary Disorder, *Phys. Rev. Lett.* **128**, 177001 (2022).
- ⁴⁷ N. F. Q. Yuan and L. Fu, Supercurrent diode effect and finite-momentum superconductors, *Proc. Natl. Acad. Sci. USA* **119**, e2119548119 (2022).
- ⁴⁸ A. Daido, Y. Ikeda, and Y. Yanase, Intrinsic Superconducting Diode Effect, *Phys. Rev. Lett.* **128**, 037001 (2022).
- ⁴⁹ H. F. Legg, D. Loss, and J. Klinovaja, Superconducting Diode Effect Due to Magnetochiral Anisotropy in Topological Insulators and Rashba Nanowires, *Phys. Rev. B* **106**, 104501 (2022).
- ⁵⁰ A. Daido and Y. Yanase, Superconducting Diode Effect and Nonreciprocal Transition Lines, *Phys. Rev. B* **106**, 205206 (2022).
- ⁵¹ C.-Z. Chen, J. J. He, M. N. Ali, G.-H. Lee, K. C. Fong, and K. T. Law, Asymmetric Josephson Effect in Inversion Symmetry Breaking Topological Materials, *Phys. Rev. B* **98**, 075430 (2018).
- ⁵² A. A. Kopasov, A. G. Kutlin, and A. S. Mel'nikov, Geometry Controlled Superconducting Diode and Anomalous Josephson Effect Triggered by the Topological Phase Transition in Curved Proximity-Induced Nanowires, *Phys. Rev. B* **103**, 144520 (2021).
- ⁵³ K. Misaki and N. Nagaosa, Theory of the Nonreciprocal Josephson Effect, *Phys. Rev. B* **103**, 245302 (2021).
- ⁵⁴ K. Halterman, M. Alidoust, R. Smith, and S. Starr, Supercurrent Diode Effect, Spin Torques, and Robust Zero-Energy Peak in Planar Half-Metallic Trilayers, *Phys. Rev. B* **105**, 104508 (2022).
- ⁵⁵ Y. Wei, H.-L. Liu, J. Wang, and J.-F. Liu, Supercurrent Rectification Effect in Graphene-Based Josephson Junctions, *Phys. Rev. B* **106**, 165419 (2022).
- ⁵⁶ Y.-M. Xie, D. K. Efetov, and K. T. Law, φ_0 -Josephson Junction in Twisted Bilayer Graphene Induced by a Valley-Polarized State, *Phys. Rev. Res.* **5**, 023029 (2023).
- ⁵⁷ Y. Zhang, Y. Gu, P. Li, J. Hu, and K. Jiang, General Theory of Josephson Diodes, *Phys. Rev. X* **12**, 041013 (2022).
- ⁵⁸ A. Soori, Nonequilibrium Josephson Diode Effect in Periodically Driven SNS Junctions, *Phys. Scr.* **98**, 065917 (2023).
- ⁵⁹ A. Soori, Anomalous Josephson Effect and Rectification in Junctions between Floquet Topological Superconductors, *Phys. E Low-Dimensional Syst. Nanostructures* **146**, 115545 (2023).
- ⁶⁰ M. Davydova, S. Prembabu, and L. Fu, Universal Josephson Diode Effect, *Sci. Adv.* **8**, eab00309 (2022).
- ⁶¹ R. S. Souto, M. Leijnse, and C. Schrade, Josephson Diode Effect in Supercurrent Interferometers, *Phys. Rev. Lett.* **129**, 267702 (2022).
- ⁶² Y. V. Fominov and D. S. Mikhailov, Asymmetric Higher-Harmonic SQUID as a Josephson Diode, *Phys. Rev. B* **106**, 134514 (2022).
- ⁶³ J.-X. Hu, Z.-T. Sun, Y.-M. Xie, and K. T. Law, Josephson Diode Effect Induced by Valley Polarization in Twisted Bilayer Graphene, *Phys. Rev. Lett.* **130**, 266003 (2023).
- ⁶⁴ R. Haenel and O. Can, Superconducting Diode from Flux Biased Josephson Junction Arrays, arXiv: 2212.02657 (2022).
- ⁶⁵ J. F. Steiner, L. Melischek, M. Trahms, K. J. Franke, and F. von Oppen, Diode Effects in Current-Biased Josephson Junctions, *Phys. Rev. Lett.* **130**, 177002 (2023).
- ⁶⁶ T. H. Kokkeler, A. A. Golubov, and F. S. Bergeret, Field-Free Anomalous Junction and Superconducting Diode Effect in Spin-Split Superconductor/Topological Insulator Junctions, *Phys. Rev. B* **106**, 214504 (2022).
- ⁶⁷ B. Lu, S. Ikegaya, P. Burset, Y. Tanaka, and N. Nagaosa, Tunable Josephson Diode Effect on the Surface of Topological Insulators, *Phys. Rev. Lett.* **131**, 096001 (2023).
- ⁶⁸ Y. Tanaka, B. Lu, and N. Nagaosa, Theory of Giant Diode Effect in *d*-Wave Superconductor Junctions on the Surface of a Topological Insulator, *Phys. Rev. B* **106**, 214524 (2022).
- ⁶⁹ H. F. Legg, K. Laubscher, D. Loss, and J. Klinovaja, Parity-Protected Superconducting Diode Effect in Topological Josephson Junctions, *Phys. Rev. B* **108**, 214520 (2023).
- ⁷⁰ A. Maiani, K. Flensberg, M. Leijnse, C. Schrade, S. Vaitiekėnas, and R. S. Souto, Nonsinusoidal Current-Phase Relations in Semiconductor-Superconductor-Ferromagnetic Insulator Devices, *Phys. Rev. B* **107**, 245415 (2023).
- ⁷¹ P. Ding, C. H. Lee, X. Wu, and R. Thomale, Diagnosis of pairing symmetry by vortex and edge spectra in kagome superconductors, *Phys. Rev. B* **105**, 174518 (2022).
- ⁷² P. Ding, T. Schwemmer, C. H. Lee, X. Wu, and R. Thomale, Hyperbolic Fringe Signal for Twin Impurity Quasiparticle Interference, *Phys. Rev. Lett.* **130**, 256001 (2023).
- ⁷³ B. Zinkl, K. Hamamoto, and M. Sigrist, Symmetry Conditions for the Superconducting Diode Effect in Chiral Superconductors, *Phys. Rev. Res.* **4**, 033167 (2022).
- ⁷⁴ J. Hu, C. Wu, and X. Dai, Proposed Design of a Josephson Diode, *Phys. Rev. Lett.* **99**, 067004 (2007).
- ⁷⁵ D. Wang, Q.-H. Wang, and C. Wu, Symmetry Constraints on Direct-Current Josephson Diodes, arXiv: 2209.12646 (2022).
- ⁷⁶ N. F. Q. Yuan and L. Fu, Zeeman-Induced Gapless Superconductivity with a Partial Fermi Surface, *Phys. Rev. B* **97**, 115139 (2018).
- ⁷⁷ N. F. Q. Yuan and L. Fu, Topological Metals and Finite-Momentum Superconductors, *Proc. Natl. Acad. Sci.* **118** (3) e2019063118 (2021).
- ⁷⁸ S. Hart, H. Ren, M. Kosowsky, G. Ben-Shach, P. Leubner, C. Brüne, H. Buhmann, L. W. Molenkamp, B. I. Halperin, and A. Yacoby, Controlled Finite Momentum Pairing and Spatially Varying Order Parameter in Proximity-Induced HgTe Quantum Wells, *Nat. Phys.* **13**, 87 (2017).
- ⁷⁹ R. S. Muller, T. I. Kamins, & M. Chan, *Device Electronics for Integrated Circuits* 3rd edn (John Wiley & Sons, Inc., 2003).
- ⁸⁰ See Supplemental Material at [URL will be inserted by publisher] for Doppler energy shift in asymmetric helical states (Sec. I), the general requirement of Josephson diode met by this states (Sec. II) scattering matrix formalism for Andreev bound states (Sec. III), the detail deduction for CPR (Sec. IV), the discussion on the topological Josephson diode (Sec. V), and the semiconductor-based JD (Sec. VI).
- ⁸¹ P. G. De Gennes, *Superconductivity of Metals and Alloys* (Benjamin, New York, 1966).
- ⁸² C. W. J. Beenakker, Universal limit of critical-current

- fluctuations in mesoscopic Josephson junctions. Phys. Rev. Lett. **67**, 3836 (1991).
- ⁸³ C. Beenakker, Three “universal” mesoscopic Josephson effects, in *Transport Phenomena in Mesoscopic Systems* Eds. Hidetoshi Fukuyama, Tsuneya Ando (Springer, 1992) pp. 235–253.
- ⁸⁴ P.-H. Fu, Y. Xu, X.-L. Yu, J.-F. Liu, and J. Wu, Electrically Modulated Josephson Junction of Light-Dressed Topological Insulators, Phys. Rev. B **105**, 064503 (2022).
- ⁸⁵ D. Zhang, M. Shi, T. Zhu, D. Xing, H. Zhang, and J. Wang, Topological Axion States in the Magnetic Insulator MnBi₂Te₄ with the Quantized Magnetoelectric Effect, Phys. Rev. Lett. **122**, 206401 (2019).
- ⁸⁶ C.-Z. Chen, J. Qi, D.-H. Xu, and X. Xie, Evolution of Berry Curvature and Reentrant Quantum Anomalous Hall Effect in an Intrinsic Magnetic Topological Insulator, Sci. China Physics, Mech. Astron. **64**, 127211 (2021).
- ⁸⁷ L. Sheng, D. N. Sheng, C. S. Ting, and F. D. M. Haldane, Nondissipative Spin Hall Effect via Quantized Edge Transport, Phys. Rev. Lett. **95**, 136602 (2005).
- ⁸⁸ H. Li, L. Sheng, and D. Y. Xing, Connection of Edge States to Bulk Topological Invariance in a Quantum Spin Hall State, Phys. Rev. Lett. **108**, 196806 (2012).
- ⁸⁹ H. Li, L. Sheng, R. Shen, L. B. Shao, B. Wang, D. N. Sheng, and D. Y. Xing, Stabilization of the Quantum Spin Hall Effect by Designed Removal of Time-Reversal Symmetry of Edge States, Phys. Rev. Lett. **110**, 266802 (2013).
- ⁹⁰ G. Tkachov, P. Burset, B. Trauzettel, and E. M. Hankiewicz, Quantum interference of edge supercurrents in a two-dimensional topological insulator, Phys. Rev. B **92**, 045408 (2015).
- ⁹¹ B. Scharf, A. Braggio, E. Strambini, F. Giazotto, and E. M. Hankiewicz, Thermodynamics in Topological Josephson Junctions, Phys. Rev. Res. **3**, 033062 (2021).
- ⁹² F. Dolcini, M. Houzet, and J. S. Meyer, Topological Josephson ϕ_0 junctions, Phys. Rev. B **92**, 035428 (2015).
- ⁹³ M. Alidoust and H. Hamzehpour, Spontaneous Supercurrent and ϕ_0 Phase Shift Parallel to Magnetized Topological Insulator Interfaces, Phys. Rev. B **96**, 165422 (2017).
- ⁹⁴ C. W. J. J. Beenakker, D. I. Pikulin, T. Hyart, H. Schomerus, and J. P. Dahlhaus, Fermion-Parity Anomaly of the Critical Supercurrent in the Quantum Spin-Hall Effect, Phys. Rev. Lett. **110**, 017003 (2013).
- ⁹⁵ G. Tkachov, Soliton Defects and Topological-Periodic Superconductivity from an Orbital Magnetic Field Effect in Edge Josephson Junctions, J. Phys. Condens. Matter **31**, 175301 (2019).
- ⁹⁶ G. Tkachov, Chiral Current-Phase Relation of Topological Josephson Junctions: A Signature of the 4π -Periodic Josephson Effect, Phys. Rev. B **100**, 035403 (2019).
- ⁹⁷ B. A. Bernevig, T. L. Hughes, and S.-C. Zhang, Quantum Spin Hall Effect and Topological Phase Transition in HgTe Quantum Wells, Science **314**, 1757 (2006).
- ⁹⁸ J. Zou and G. Jin, Exchange-Field-Modulated $0-\pi$ Transition and Chiral Edge Supercurrents in a Superconductor/Ferromagnetic Topological Insulator/Superconductor Junction, Phys. Rev. B **85**, 134528 (2012).
- ⁹⁹ Y. Xu, S. Uddin, J. Wang, Z. Ma, and J.-F. Liu, Electrically Modulated SQUID with a Single Josephson Junction Coupled by a Time Reversal Breaking Weyl Semimetal Thin Film, Phys. Rev. B **97**, 035427 (2018).
- ¹⁰⁰ P.-H. Fu, J. Wang, J.-F. Liu, and R.-Q. Wang, Josephson Signatures of Weyl Node Creation and Annihilation in Irradiated Dirac Semimetals, Phys. Rev. B **100**, 115414 (2019).
- ¹⁰¹ A. Rasmussen, J. Danon, H. Suominen, F. Nichele, M. Kjaergaard, and K. Flensberg, Effects of Spin-Orbit Coupling and Spatial Symmetries on the Josephson Current in SNS Junctions, Phys. Rev. B **93**, 155406 (2016).
- ¹⁰² J.-F. Liu and K. S. Chan, Relation between Symmetry Breaking and the Anomalous Josephson Effect, Phys. Rev. B **82**, 125305 (2010).
- ¹⁰³ T. Yokoyama, M. Eto, and Y. V. Nazarov, Josephson Current through Semiconductor Nanowire with Spin-Orbit Interaction in Magnetic Field, J. Phys. Soc. Japan **82**, 054703 (2013).
- ¹⁰⁴ T. Yokoyama, M. Eto, and Y. V. Nazarov, Anomalous Josephson Effect Induced by Spin-Orbit Interaction and Zeeman Effect in Semiconductor Nanowires, Phys. Rev. B **89**, 195407 (2014).
- ¹⁰⁵ C.-X. Liu, X.-L. Qi, X. Dai, Z. Fang, and S.-C. Zhang, Quantum Anomalous Hall Effect in $Hg_{1-y}Mn_yTe$ Quantum Wells, Phys. Rev. Lett. **101**, 146802 (2008).
- ¹⁰⁶ S. Hart, H. Ren, T. Wagner, P. Leubner, M. Mühlbauer, C. Brüne, H. Buhmann, L.W. Molenkamp, and A. Yacoby, Induced superconductivity in the quantum spin Hall edge, Nat. Phys. **10**, 638 (2014).
- ¹⁰⁷ J. Chen, W. Xu, Z. Tan, Z. Pan, P. Zhu, Z.-M. Liao, and D. Yu, Superconducting Proximity in Intrinsic Magnetic Topological Insulator MnBi₂Te₄-NbN Hybrid Device Modulated by Coulomb Blockade Effect, Nano Lett. **22**, 6484 (2022).
- ¹⁰⁸ W.-Z. Xu, C.-G. Chu, Z.-C. Pan, J.-J. Chen, A.-Q. Wang, Z.-B. Tan, P.-F. Zhu, X.-G. Ye, D.-P. Yu, and Z.-M. Liao, Proximity-Induced Superconducting Gap in the Intrinsic Magnetic Topological Insulator MnBi₂Te₄, Phys. Rev. B **105**, 184515 (2022).
- ¹⁰⁹ C. Huang, A. Narayan, E. Zhang, X. Xie, L. Ai, S. Liu, C. Yi, Y. Shi, S. Sanvito, and F. Xiu, Edge Superconductivity in Multilayer WTe₂ Josephson Junction, Natl. Sci. Rev. **7**, 1468 (2020).
- ¹¹⁰ F. Lüpke, D. Waters, S. C. de la Barrera, M. Widom, D. G. Mandrus, J. Yan, R. M. Feenstra, and B. M. Hunt, Proximity-Induced Superconducting Gap in the Quantum Spin Hall Edge State of Monolayer WTe₂, Nat. Phys. **16**, 526 (2020).
- ¹¹¹ G. De Simoni, F. Paolucci, C. Puglia, and F. Giazotto, Josephson Field-Effect Transistors Based on All-Metallic Al/Cu/Al Proximity Nanojunctions, ACS Nano **13**, 7871 (2019).
- ¹¹² Z. Xu, W. Chen, J. Huang, W. Tian, S. Chen, W. Yue, T. Chi, Y.-Y. Lyu, H. Sun, Y.-L. Wang, G. Sun, J. Chen, B. Jin, S.-L. Li, H. Yuan, J. Li, D. Koelle, R. Kleiner, H. Wang, and P. Wu, Vertical Josephson Field-Effect Transistors Based on Black Phosphorus, Appl. Phys. Lett. **119**, 072601 (2021).